Inverse energy cascade in a turbulent round jet

M. Yu. Hrebtov,[1] B. B. Ilyushin,[1,2] and D. V. Krasinsky[1,2]
[1]*Kutateladze Institute of Thermophysics, SB RAS, Novosibirsk, Russia*
[2]*Nuclear Safety Institute, RAS, Moscow, Russia*

(Received 10 March 2009; revised manuscript received 31 August 2009; published 25 January 2010)

Large eddy simulation of turbulent free round jet has been performed to study statistical properties of turbulence, including third-order structure functions. It has been shown the presence of a zone within the jet initial region where the spectral flux of turbulent energy is directed from smaller scales toward larger ones and the longitudinal third-order structure function becomes positive. Energy spectra calculated in this zone demonstrate the $E(k) \sim k^{-3}$ law specific for two-dimensional turbulence.

DOI: 10.1103/PhysRevE.81.016315 PACS number(s): 47.27.−i

I. INTRODUCTION

Among a lot of works devoted to investigation of the turbulent flows structure, research on mechanisms of energy transformation in turbulent vortices holds a place. Known concepts about the turbulent energy cascade from large to smaller-size eddies, based on Richardson model and developed by Kolmogorov [1], have been validated in experimental and theoretical works. According to Kolmogorov's "4/5" law [2], the third-order longitudinal velocity structure function defined as $D_{LLL}(\ell) \equiv \langle [u_L(M') - u_L(M)]^3 \rangle$ should stay negative in three-dimensional homogeneous isotropic turbulence [3] (hereinafter ℓ denotes the distance between points M' and M, u_L is the instantaneous longitudinal velocity component, and the angular brackets $\langle \cdot \rangle$ denote ensemble averaging). This feature is closely related to the concept that turbulent pulsations of a given scale should on average transfer energy toward pulsations of smaller scales and, accordingly, take energy from larger-scale pulsations [3]. Indeed, various experimental data and numerical simulations detect negative values of D_{LLL} in developed three-dimensional turbulent flows, see, e.g., [4–6].

Energy cascade directed from smaller scales toward larger ones, and positiveness of longitudinal velocity structure function, $D_{LLL} > 0$, are typical features of two-dimensional turbulence [7]. These phenomena, caused by the absence of the vortex tube stretching mechanism [8], have also been observed in three-dimensional flows with anisotropy stemming from stratification or rotation (see, e.g., [9,10]). In the latter case turbulence can be considered as quasi-two-dimensional due to effect of suppression of turbulent fluctuations in the direction of centrifugal force or buoyancy force in stable stratification. As observed in these flows, quasi-two-dimensional vortex structures are growing there by involving the fluid from nearby layers and by merging ("pairing") with other vortices as well.

Experimental examination of free submerged round jet flow based on particle image velocimetry (PIV) technique has been conducted in [11,12] where detailed database on the turbulent statistical properties has been obtained. Periodic formation of vortices that evolve from the nozzle edge downstream along the jet shear layer has been observed in experiment. At the distance of about one to two nozzle diameters these vortices merge, thus forming the long-living toroidal vortex structures [12]. Technique used in [11,12] has allowed to evaluate the field of $D_{LLL}(\ell)$ from PIV data on submerged round jet flow at Re=28 000—actually the statistical moments of the longitudinal velocity derivative computed as finite differences on uniform grid with $\ell = 0.85$ mm have been obtained in experiment. This quantity presented hereinafter in the "normalized" form as $D_{LLL}(\ell)/\ell$ (to exclude the linear dependence of D_{LLL} on ℓ, see, e.g., [2,3,8,18]) appeared to be positive at the outer side of the jet shear layer—see Fig. 1 (left, kindly provided by Alekseenko *et al.* [20]). Notwithstanding some noticeable noise arising from experimental error, zones where $D_{LLL} > 0$ can be seen extending from the nozzle edge to ~5 nozzle diameters downstream.

Large Eddy Simulation (LES) approach (see, e.g., [13]) has for the past decade proven to be the "mainstream" line in research of turbulence modeling. In LES the major part of turbulent motion is resolved "directly" whereas the effects of remaining scales smaller than the computational grid size (filterwidth) are accounted in a subgrid-scale (SGS) model. In the previous works of authors [14,15] some results of LES study on dynamics and vortex structure of free turbulent submerged round jet at Re=25 000 have been reported. In the

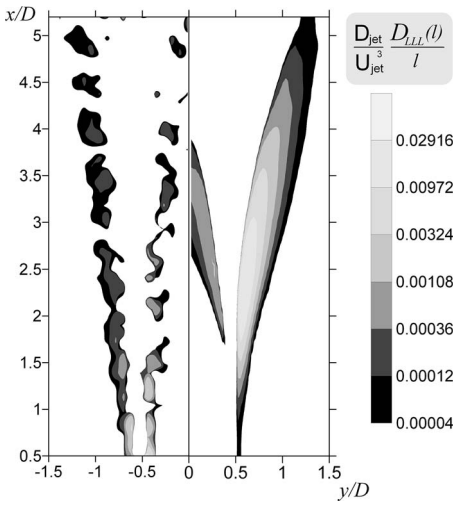

FIG. 1. Distributions of dimensionless structure function $D_{LLL}/(\ell U_{\text{jet}}^3/D_{\text{jet}})$ obtained in experiment [11,12,20] (left) and in LES (right) in longitudinal section of the jet (only positive values shown).

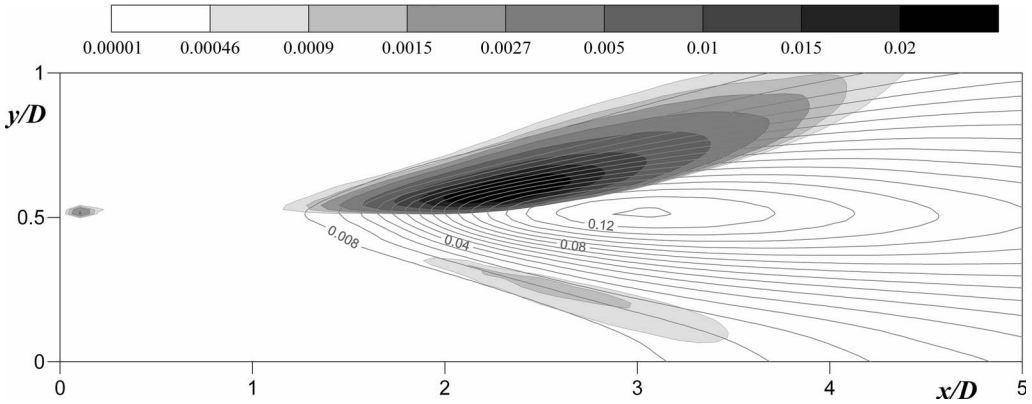

FIG. 2. LES fields of dimensionless structure function $D^*_{LLL} \equiv D_{LLL}/(\ell U^3_{\text{jet}}/D_{\text{jet}})$ (shaded contours, only positive values shown) and the turbulent kinetic energy (isocurves).

present paper, further results of LES of this jet are demonstrated, with emphasis on statistical properties of turbulent field, including analysis of structure functions.

II. LES OF FREE ROUND SUBMERGED TURBULENT JET: RESULTS AND DISCUSSION

Free axisymmetric submerged jet discharged from the profiled nozzle with low level of turbulent pulsations intensity (~2%) is considered. The jet Reynolds number was Re=25 000 based on the nozzle diameter $D_{\text{jet}}=10$ mm and the mean flowrate $U_{\text{jet}}=1.9$ m/s in water. A bluff-body with outer diameter $D_b=54.2$ mm was mounted over the nozzle edge. Smagorinsky SGS model with coefficient $C_S=0.175$ has been used in LES. To prescribe the mean axial velocity profile at the jet inlet, the hyperbolic tangent law (close to stepwise profile) corresponding to experimental data has been applied. More details on boundary conditions as well as numerical algorithm are given in [14]. Fields of mean velocity and r.m.s. of its pulsations, turbulent kinetic energy and its spectra, other turbulent quantities and vortex structure of the jet flow obtained in LES have been reported in [14,15]. Comparison of LES results with experimental data [12] has shown their agreement [14,15].

With axisymmetric topology of the flow taken into account, time-averaging of instantaneous LES data has been superimposed with averaging in circumferential direction during computation of statistical moments in the present work (as well as in [14,15]). To validate this type of averaging, comparison between the results averaged with the use of additional averaging in circumferential direction, and the results averaged without it but with significantly larger sampling period in time, has been performed for the distributions of statistical moments up to fourth order and also structure functions. This comparison has shown that both types of averaging produce almost identical results.

LES predictions have also confirmed that, in accordance with [3], the higher statistical moment is to be computed the larger sampling amount is needed. For example, for the first- and second-order moments of velocity pulsations several thousand of instantaneous flowfield samples were sufficient, however proper calculation of the third- and fourth-order moments has required up to 10^5 samples.

It is known that in calculation of statistical moments of velocity derivative of n-th order $\partial^n u_j/\partial x_j^n$, the contribution of small scales grows with n increasing [3]. As soon as these "small" scales reach SGS level and are cutoff in LES, care should be taken that the effect of this cutoff on evaluation of statistical moments of velocity derivative remains insignificant. Therefore, a series of LES runs have been conducted and structure functions of third order have been calculated on a sequence of refined grids. Comparative analysis has indicated almost no changes in the obtained normalized structure functions starting from resolution of $360\times132\times48$ grid, with this the sampling time period was about 10 s of jet evolution. Similarly to PIV data processing (Fig. 1, left), in LES the normalized third-order longitudinal velocity structure function was computed according to its finite difference form: $D_{LLL}/\ell \approx \langle(\delta u_L)^3\rangle/\delta x$, where δx is the grid cell size in longitudinal direction and δu_L is the corresponding velocity increment.

LES predictions have revealed the presence of zones where D_{LLL} takes positive values, see Fig. 1 (right) and Fig. 2 (shaded contours indicate $D_{LLL}>0$, and iso-curves represent the turbulent kinetic energy field in Fig. 2). These zones are located within the jet initial region at the distance of $1-5D_{\text{jet}}$ from the nozzle orifice, where intense vortex formation takes place inside the mixing layers. These mixing layers undergoing the mean velocity shear are extending from the nozzle edge to their convergence at the distance of about $4-5D_{\text{jet}}$ [16]. Such processes of vortex evolution are demonstrated by visualization of the jet vortex structure shown in Fig. 3 as a typical instantaneous field of λ_2 criterion (its negative values, $\lambda_2<0$, identify locations of vortical motion). This widely used criterion is based on identification of a vortex core in an incompressible flow by the sign of second eigenvalue λ_2 (assuming arrangement $\lambda_1\geq\lambda_2\geq\lambda_3$) of sym-

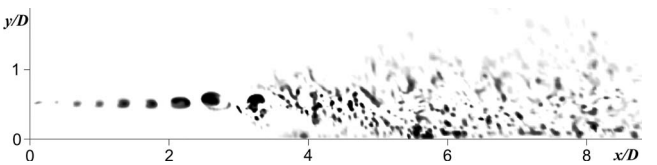

FIG. 3. Typical vortex structure of the jet visualized with λ_2 criterion (shaded pixels indicate $\lambda_2<0$).

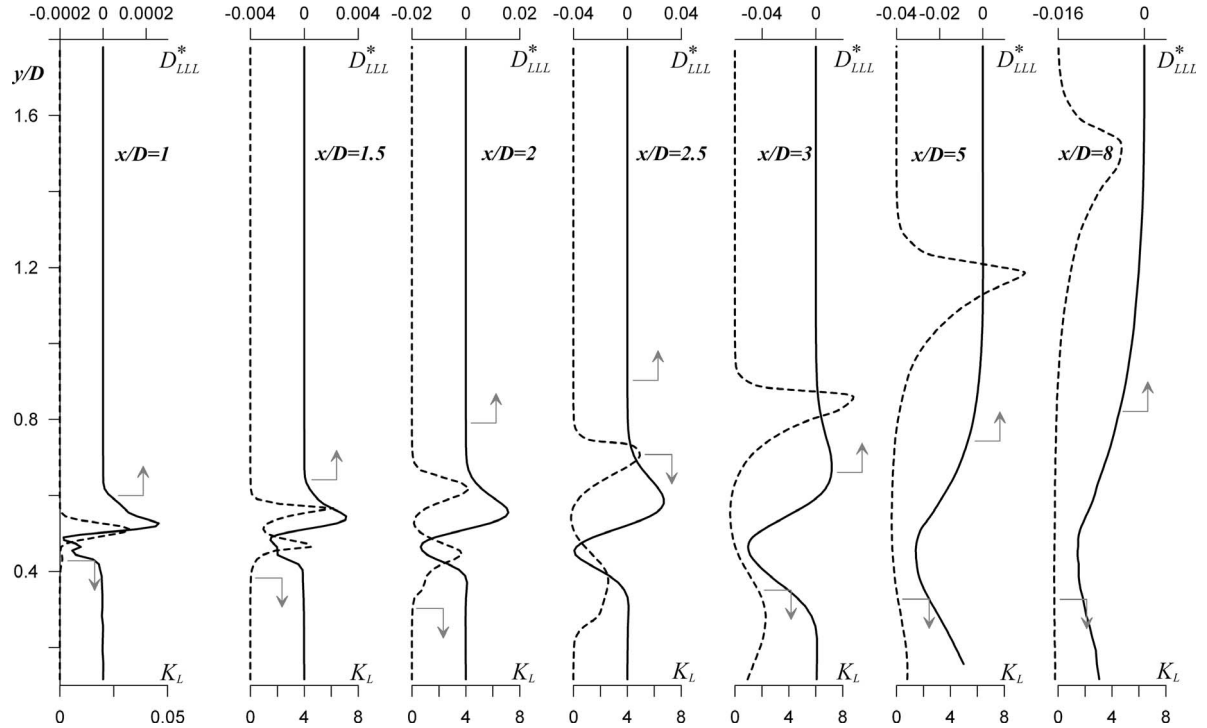

FIG. 4. Radial profiles of dimensionless structure function D^*_{LLL} (solid lines) and flatness K_L (dashed lines) at several cross-sections of the jet.

metric tensor $\mathbf{S}^2+\mathbf{\Omega}^2$, where $\mathbf{S}$ and $\mathbf{\Omega}$ are, respectively, the symmetric and antisymmetric components of the velocity gradient tensor (for details on λ_2-criterion derivation see, e.g., [17]). Maximum of D_{LLL}/ℓ field (its nondimensional values $D^*_{LLL} \equiv D_{LLL}/(\ell U^3_{\text{jet}}/D_{\text{jet}})$ are presented in Fig. 2, as well as in Figs. 4 and 5) is located near the outer side of mixing layer at the distance of $\sim 2.5 D_{\text{jet}}$, with this D_{LLL}/ℓ values in the "lower" zone (where $D_{LLL}>0$) are substantially smaller than in the "upper" one.

Radial profiles of dimensionless structure function D^*_{LLL} and the flatness coefficient of longitudinal velocity $K_L = \langle u_L^4 \rangle / \langle u_L^2 \rangle^2 - 3$ obtained in LES are shown in Fig. 4. Locations of maxima in K_L profile indicate the regions where the processes of undisturbed flow involvement into the mixing layer are significant—thus, indicating the mixing layer boundaries. It can be seen that within the jet region $x/D_{\text{jet}} < 1.5$ the zones where $D_{LLL}>0$ are located nearby the maxima of flatness coefficient K_L, i.e., at the mixing layer boundaries. However, from the distance of $x/D_{\text{jet}} \sim 2$ and downstream, the intensity of turbulent pulsations in the mixing layer becomes significant (see turbulent kinetic energy (TKE) distribution in Fig. 2)—the zones of positive D_{LLL} appear to be inside the mixing layer. Up to the moment of convergence of mixing layers evolved from the nozzle edge,

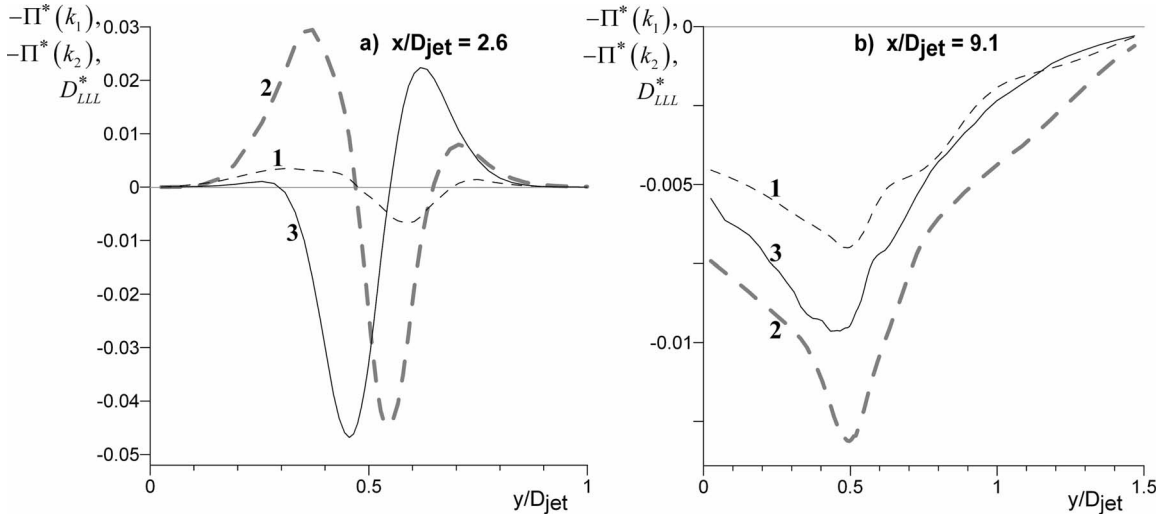

FIG. 5. Radial profiles of dimensionless turbulent energy fluxes $-\Pi^*(k_1)$ (curve 1), $-\Pi^*(k_2)$ (curve 2), and dimensionless structure function D^*_{LLL} (curve 3), at the jet sections: (a) $x/D_{\text{jet}}=2.6$; (b) $x/D_{\text{jet}}=9.1$

the processes of undisturbed flow involvement into the mixing layer by vortex structures occur both from outer side of the jet as well as from the jet axis. This causes the presence of two maxima in K_L profile. Downstreams, with mixing layer growing, the distance between two maxima in K_L profile is increasing with amplitude of "lower" K_L maximum (i.e., one moving toward the axis) decreasing. At the distance of $\sim 5D_{\text{jet}}$ from the nozzle orifice, where the mixing layers converge, it is already indistinguishable. At this point the zones of positive D_{LLL} values are also vanishing.

III. RETRIEVAL OF TURBULENT ENERGY FLUX AND ENERGY SPECTRA FROM LES DATA

Because the sign of the structure function D_{LLL} is closely related to the direction of turbulent energy cascade over the scales, the obtained effect of presence of a zone where $D_{LLL}>0$, mentioned above, gives grounds to expect that mechanisms of turbulent energy cascade exhibit "nonstandard" features in this zone. Analysis presented below allowed us to verify this assertion via the straightforward computation of turbulent energy flux.

On the basis of the low-pass filtering applied to the Navier-Stokes equations, the following scale-by-scale energy budget equation has been derived in [18] without the use of the local homogeneity and isotropy hypotheses:

$$\partial_t E_k + \Pi_k = -2\nu\Omega_k + F_k, \tag{1}$$

where E_k is the cumulative energy contained between wave numbers 0 and k, Π_k is the turbulent energy flux through the wave number k (or the scale $2\pi/k$) appearing due to nonlinear interactions, ν is the kinematic viscosity coefficient, Ω_k is the cumulative enstrophy contained between wave numbers 0 and k, and F_k is the cumulative energy injection by external force at these scales. Detailed derivation of Eq. (1) has been given in [18]. It should be noted that, according to Taylor's frozen turbulence hypothesis applied to the steady-state axisymmetric jet flow considered herein, ensemble-averaging operation can be substituted with time-averaging. The sign of Π_k indicates the direction of energy flux through a given wave number k (or a scale $2\pi/k$), i.e., with $\Pi_k>0$ the energy flux is directed from smaller wave numbers toward larger ones, and vice versa. The flux Π_k is determined as [18]

$$\Pi_k = \langle \vec{u}_k^{<} \cdot (\vec{u}_k^{<} \cdot \nabla \vec{u}_k^{>}) \rangle + \langle \vec{u}_k^{<} \cdot (\vec{u}_k^{>} \cdot \nabla \vec{u}_k^{>}) \rangle, \tag{2}$$

where $\vec{u}_k^{<}$ is the low-pass filtered velocity and $\vec{u}_k^{>}$ is the high-pass filtered velocity. Taking into account that $\vec{u}_k^{>} = \vec{u} - \vec{u}_k^{<}$, only low-pass filtering of LES data is enough to compute Π_k according to formulation (2).

The spherical "top-hat" filter with radius R (half-width of the filter) has been used for spatial averaging of LES data during the procedure of low-pass filtering. Figure 5 demonstrates radial distributions of $-\Pi^*(k) \equiv -\Pi_k/(U_{\text{jet}}^3/D_{\text{jet}})$ (i.e., dimensionless energy flux displayed with inverse sign) obtained from Eq. (2) at the jet cross-sections of $x/D_{\text{jet}}=2.6$ where D_{LLL} has positive values [Fig. 5(a)], and also $x/D_{\text{jet}}=9.1$ where D_{LLL} stays negative [Fig. 5(b)]. With this, the energy flux has been computed at two wave numbers $k_1=2\pi/D_{\text{jet}}$ (corresponding to filter radius $R_1=0.5D_{\text{jet}}$) and $k_2=4\pi/D_{\text{jet}}$ ($R_2=0.25D_{\text{jet}}$)—see curves 1 and 2 in Fig. 5. Together with these curves, radial profiles of dimensionless structure function D_{LLL}^* (curve 3) are shown in Fig. 5. It should be noted that the structure function D_{LLL} contains information on turbulent energy transfer over all scales on average, whereas Π_k corresponds to energy flux through only a given scale (wave number k). Therefore comparative analysis of D_{LLL} and Π_k behavior can only be qualitative. It can be seen from Fig. 5(a) that at cross-section $x/D_{\text{jet}}=2.6$ where radial profile of D_{LLL}^* changes its sign twice with distance y varying, both profiles of $-\Pi^*(k_1)$ and $-\Pi^*(k_2)$ change the sign accordingly and are closely following the behavior of D_{LLL}^* distribution. Similarly at cross-section $x/D_{\text{jet}}=9.1$ where $D_{LLL}<0$, both $-\Pi^*(k)$ profiles are also negative (i.e., energy flux Π_k is positive) and locations of extrema in all three profiles almost coincide—see Fig. 5(b). The latter observation validates correlation between the structure function D_{LLL} and the energy flux Π_k. Thus, the straightforward computations of turbulent energy flux have confirmed that in the zone where positive values of D_{LLL} are observed, the energy flux estimated for at least two wave numbers $k_1=2\pi/D_{\text{jet}}$ and $k_2=4\pi/D_{\text{jet}}$ is inversely directed—from smaller scales toward larger ones.

In further study of turbulent energy cascade mechanisms developed in the free round jet flow, power spectra of turbulent energy have been computed in the jet cross-sections $x/D_{\text{jet}}=2.5$, 3, 5, and 8, see Fig. 6. It can be seen that in section $x/D_{\text{jet}}=2.5$ [Fig. 6(a)] where D_{LLL}/ℓ values are near maximum, the spectra inside mixing layer (at points $y/D_{\text{jet}}=0.44-0.6$) obey the $E(k)\sim k^{-3}$ law. Outside the mixing layer, the spectra are less developed as the turbulent intensity is substantially lower there than inside mixing layer. Downstreams, as the mixing layer evolves, the spectra inside it transform to Kolmogorov law. Indeed, from Fig. 6(b), it can be seen that at $x/D_{\text{jet}}=3$ the spectra inside mixing layer approach the $E(k)\sim k^{-5/3}$ law while at the outer bound of mixing layer (at $y/D_{\text{jet}}=0.60-0.66$) the spectra still follow the $E(k)\sim k^{-3}$ law.

At the distance of $5D_{\text{jet}}$ from the nozzle and downstreams, the inertial range with Kolmogorov $E(k)\sim k^{-5/3}$ spectrum becomes more pronounced within the jet—see Fig. 6(c). Further downstreams at $8D_{\text{jet}}$ from the nozzle where the developed jet region takes place [see Fig. 6(d)] the spectra across the whole jet width (from axis to $y/D_{\text{jet}}=0.76$) merge toward universal Kolmogorov law. It should be noted that the $E(k)\sim k^{-3}$ spectrum is typical for two-dimensional turbulence with enstrophy cascade range (contrary to Kolmogorov's inertial range of energy cascade in three-dimensional turbulence). Presented LES results have demonstrated that this kind of spectrum is formed in the mixing layer at the jet initial region. Downstreams, the spectrum undergoes transformation approaching the universal Kolmogorov $\sim k^{-5/3}$ law [see Figs. 6(a)–6(d)].

A reverse process has been reported in the work on numerical modeling of two-dimensional turbulence [19] when an initial distribution of turbulent pulsations prescribed according to Kolmogorov $E(k)\sim k^{-5/3}$ spectrum has later evolved to the $E(k)\sim k^{-3}$ form. During this the development of self-similar vortex structures via merging of smaller vortices in the inverse energy cascade—transferring energy to-

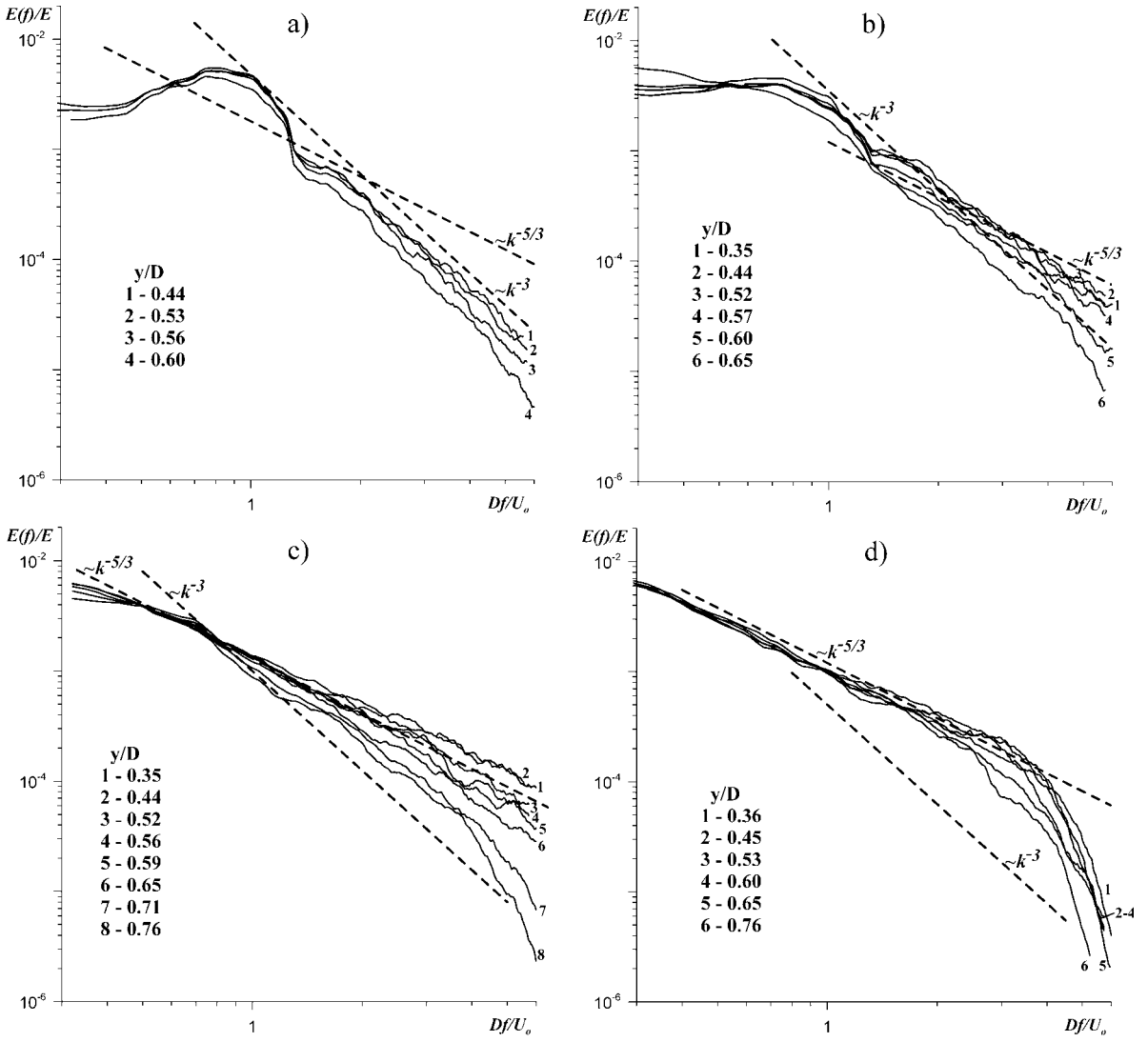

FIG. 6. Power spectra of turbulent energy at several points across the jet, in sections (a) $x/D_{\text{jet}}=2.5$, (b) 3.0, (c) 5.0, and (d) 8.0.

ward larger scales—has been observed in [19].

Energy spectrum with $E(k)\sim k^{-3}$ range typical for two-dimensional turbulence indicates that the mechanisms of vortex structures' growth (by their merging and by involving the ambient fluid) are predominant over the mechanisms of vortex structures' decreasing (caused by vortex tube stretching and by viscous dissipation). A distinctive feature of this kind of turbulent field is that its spectral energy flux is inversely directed—from smaller scales to larger ones. Apparently, this causes the positiveness of the third-order longitudinal velocity structure function at the mixing layer bounds within the jet initial region.

IV. CONCLUSIONS

On the basis of LES of essentially three-dimensional flow—free round submerged turbulent jet—it has been found the presence of a region where turbulence dynamics exhibit two-dimensional features that could not be caused by external anisotropy conditions (like stratification or rotation). LES predictions have demonstrated that inside this region: the third-order longitudinal velocity structure function takes positive values, the turbulent energy flux estimated from LES is directed from smaller scales toward larger ones, and the power spectrum of turbulent fluctuations follows the $E(k)\sim k^{-3}$ law. The latter indicates that vortex dynamics in this region is governed by mechanisms specific for two-dimensional turbulence when the growth of vortex structures caused by their merging and by involving the ambient fluid is predominant over the effects of the vortex tube stretching and the viscous dissipation. Positive D_{LLL} values and inverse direction of turbulent energy flux Π_k are the immediate consequences of such kind of dynamics. It may also be suggested that similar "anomalous" regions with inverse flux of turbulent energy can occur in some other turbulent flows where the formation of large-scale quasi-two-dimensional vortex structures is governed by mechanisms of the vortex merging and the involvement of ambient fluid while the effects of the viscous dissipation and the vortex tube stretching remain insignificant.

ACKNOWLEDGMENTS

Authors wish to thank their colleagues S. V. Alekseenko, A. V. Bilsky, V. M. Dulin, and D. M. Markovich for the fruitful discussions and the provided experimental data (Fig. 1, left). Computations were performed using the supercomputers MVS-6000 and MVS-100k (Joint Supercomputer Center of RAS, Moscow). The work has been supported by the Russian Foundation for Basic Research (Grant No. 06-01-00724-a) and by the Grant for Leading Research Schools (Grant No. HII-6749.2006.8).

[1] A. N. Kolmogorov, Dokl. Akad. Nauk SSSR **30**, 9 (1941); Proc. R. Soc. London, Ser. A **434**, 9 (1991).
[2] A. N. Kolmogorov, Dokl. Akad. Nauk SSSR **32**, 16 (1941); Proc. R. Soc. London, Ser. A **434**, 15 (1991).
[3] A. S. Monin and A. M. Yaglom, *Statistical Fluid Mechanics: Mechanics of Turbulence* (MIT Press, Cambridge, 1975), Pt. 2.
[4] Francois N. Frenkiel, and Philip S. Klebanov, Phys. Fluids **10**, 507 (1967).
[5] J. Schumacher, K. R. Sreenivasan, and P. K. Yeung, Phys. Fluids **15**, 84 (2003).
[6] Siegfried Grossmann, Detlef Lohse, and Achim Reeh, Phys. Rev. Lett. **77**, 5369 (1996).
[7] G. Boffetta, A. Celani, and M. Vergassola, Phys. Rev. E **61**, R29 (2000).
[8] M. Lesieur, *Turbulence in Fluids* (Kluwer, Dordrecht, 1997).
[9] Charles N. Baroud, Brendan B. Plapp, and Harry L. Swinney, Phys. Fluids **15**, 2091 (2003).
[10] Joseph M. Prusa, Piotr K. Smolarkiewicz, and Andrzej A. Wyszogrodzki, SIAM News 32 (7) (1999).
[11] S. V. Alekseenko, A. V. Bilsky, V. M. Dulin, B. B. Ilyushin, and D. M. Markovich, Proceedings of the Fourth International Symposium on Turbulence and Shear Flow Phenomena (TSFP-4), Williamsburg, VA, 27–29 June 2005 (unpublished), Vol. 2, pp. 605–610.
[12] S. V. Alekseenko, A. V. Bilsky, and D. M. Markovich, Instrum. Exp. Tech. **47**, 703 (2004).
[13] P. Sagaut, *Large Eddy Simulation for Incompressible Flows: An Introduction* (Springer-Verlag, Berlin, 2001).
[14] B. B. Ilyushin and D. V. Krasinsky, Thermophys. Aeromechanics **13**, 43 (2006).
[15] B. B. Ilyushin, D. V. Krasinsky, and M. Yu. Hrebtov, *Proceedings of the Thirteenth International Conference on the Methods of Aerophysical Research (ICMAR-2007)*, edited by V. M. Fomin (Parallel, Novosibirsk, 2007), Pt. III, pp. 141–146.
[16] A. S. Ginevsky, Ye. V. Vlasov, and R. K. Karavosov, *Acoustic Control of Turbulent Jets* (Fizmatlit, Moscow, 2001) (in Russian).
[17] J. Jeong and F. Hussain, J. Fluid Mech. **285**, 69 (1995).
[18] U. Frisch, *Turbulence: The legacy of A. N. Kolmogorov* (Cambridge University Press, Cambridge, England, 1995).
[19] V. Borue, Phys. Rev. Lett. **72**, 1475 (1994).
[20] S. V. Alekseenko, A. V. Bilsky, V. M. Dulin, and D. M. Markovich (private communication).